31st Congress of the International Council of the Aeronautical Sciences

Belo Horizonte, Brazil; September 09-14, 2018

# INVISCID AND VISCOUS FLOW MODELING FOR FAST TRANSONIC FLUTTER CALCULATIONS

**H. Güner*** , **G. Dimitriadis*** , **V. E. Terrapon***

***Aerospace and Mechanical Engineering Department, University of Liège, Quartier Polytech 1, Allée de la Découverte 9, 4000 Liège, Belgium**

**Keywords:** *unsteady aerodynamics, RANS, dynamic mode decomposition, transonic, flutter*

## Abstract

*Transonic aeroelastic analysis at the design level relies on linear panel methods, such as the Doublet Lattice approach, usually after application of transonic corrections. The results from these calculations cannot predict shock motion, shock-boundary layer interactions and the effects of such phenomena on flutter behavior, even after corrections are applied, since the latter are generally quasi-steady. This paper proposes a higher-fidelity approach that involves the solutions of the flow equations in order to obtain the unsteady flow response to relatively small amplitude periodic deformations of a structure over a large range of oscillation frequencies. The main idea is to perform a few high-fidelity CFD simulations, such as Euler or RANS simulations, with an imposed structural deformation at selected oscillation frequencies so as to capture the most dominant nonlinear dynamic modes of the flow response. These fluid dynamic modes are then interpolated to estimate the flow response for any other oscillation frequency. The methodology can then be used to obtain a frequency-domain generalized aerodynamic force matrix, and stability analysis can be performed using standard flutter calculation methods such as the p-k method. The present methodology provides a very good estimate of the flutter boundary for the 2D Isogai airfoil validation case, but at much lower computational cost than the traditional higher-fidelity Fluid-Structure Interaction (FSI) simulations.*

## 1 Introduction

The prediction of transonic flutter is of great importance to aircraft design as modern aircraft commonly fly at transonic conditions. However, the computation of the aeroelastic response of aircraft wings or control surfaces is challenging in this regime because unsteady transonic flows are characterized by aerodynamic nonlinearities such as moving shocks, shock-boundary layer interaction, and flow separation. These complex nonlinear phenomena can result in unwanted aeroelastic effects and limit the performance of aircraft [1, 2].

This paper presents a novel unsteady aerodynamic modeling methodology with higher fidelity than the linear panel methods that are commonly used in preliminary design, especially at transonic conditions where it takes into account complex aerodynamic nonlinearities (e.g., moving shocks and their interactions with the viscous boundary layer). Furthermore, the computational cost of the new methodology is low enough to be applied to aeroelastic calculations. It relies only on a limited number of reference fluid dynamic modes, which are extracted from a few unsteady RANS (or Euler) simulations. These fluid dynamic modes can also be obtained directly and at lower cost by Harmonic Balance (HB) simulations [3, 4]. Another advantage is that the present methodology can be used with standard flutter analysis techniques such as the *p-k* method [5] to find the flutter speed of a system and characterize its subcritical behavior.

The paper is organized as follows. Section 2 describes the proposed methodology. Each step of the methodology is illustrated in the case of a pitching airfoil in the transonic flow regime in Section 3. The present approach is then used to calculate the transonic flutter characteristics of the 2D Isogai airfoil validation case in Section 4. Finally, the main results are summarized and discussed in Section 5.

## 2 Methodology

The goal of the methodology is to provide the flow response to small amplitude periodic deformations of a structure as a function of the oscillation frequency for given flow conditions (Reynolds number $Re$ and Mach number $M$).

The main practical steps of the methodology are summarized as follows:

**1.** The first step is to carry out a few unsteady high-fidelity simulations (Euler or RANS) in order to obtain the flow response to an imposed small amplitude periodic structural deformation at two nearby oscillation frequencies and for given flow conditions. These reference frequencies are chosen knowing that flutter typically occurs at non-dimensional reduced frequencies of the order of 0.1 in most transonic flutter problems encountered in aircraft wings or control surfaces [1]. Additionally, the methodology has to accurately capture the unsteady nonlinear aerodynamic effects over a certain range of frequencies. The choice of the reference frequencies can be verified a posteriori based on the analysis results. This aspect is discussed in more details in Güner *et al.* [6]

**2.** The resulting unsteady flow fields are processed using the Dynamic Mode Decomposition (DMD) [7, 8] in order to extract the most relevant dynamic modes of the flow response at the reference frequencies. The first fluid dynamic modes are usually sufficient to capture the flow dynamics with good accuracy for attached inviscid flows as explained in Güner *et al.* [9, 6]. This assumption will be tested in the case of viscous flows in Section 3.

**3.** The present methodology proposes to interpolate these reference fluid dynamic modes in order to compute the entire flow fields to an imposed periodic deformation of the structure at any oscillation frequency.

The following section illustrates each step of the methodology for the case of a 2D NACA airfoil. The dynamic mode interpolation methodology can be extended to three-dimensional cases as described in Güner *et al.* [6].

## 3 Turbulent transonic flow over a pitching airfoil

The 2D transonic flow over a NACA 64A010 airfoil pitching around its quarter-chord point is used as a test case, based on the experiment by Davis [10]. This configuration has been chosen as it also enables the study of shocks that move due to structural oscillations. In the experimental conditions, the Reynolds number $Re$ based on the chord $c$ is $12.56 \times 10^6$ and the free-stream Mach number $M$ is 0.796. The pitching motion is specified as

$$\alpha(\tau) = \bar{\alpha} + \hat{\alpha}\sin(k\tau), \qquad (1)$$

where $\alpha(\tau)$ is the variation of the angle of attack with non-dimensional time $\tau = tU_\infty/b$, $U_\infty$ is the free-stream velocity, $b = c/2$, $\bar{\alpha}$ is the mean angle of attack, $\hat{\alpha}$ is the pitching amplitude, and the forcing non-dimensional reduced frequency is defined as $k = \omega b/U_\infty$ with $\omega$ the angular frequency. Unless otherwise specifically mentioned, all following results are obtained for $\bar{\alpha} = 0°$, $\hat{\alpha} = 1.01°$ and $k = 0.202$. Massive flow separation does not occur as the mean angle of attack and pitching amplitude are small.

In the following, each step of the methodology is described:

**1.** An unsteady simulation is carried out by solving the unsteady RANS equations with the one-equation Spalart-Allmaras (SA) turbulence

model, in which the transported quantity is directly linked to the turbulent eddy viscosity. The SA turbulence model is convenient for external aerodynamic flows such as the flow around an airfoil [11]. The open-source CFD code SU2 [12, 13, 14] is used in this work.

The structured C-type mesh shown in Fig. 1 consists of 46224 quadrilateral elements with 300 points around the airfoil and 109 points in the normal direction. The flow is turbulent and a boundary layer develops over the surface of the airfoil. The spacing at the wall is set so that $y^+$ is less than 1 in order to properly capture the boundary layer. The time-accurate simulation uses 25 time steps per period of oscillation to capture the relevant time scales, and the calculation is run until a periodic state has been reached to eliminate transient effects.

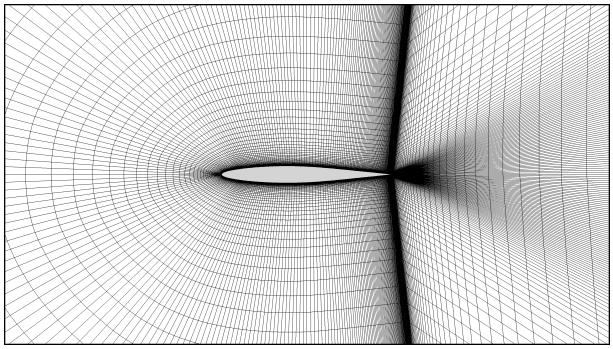

Fig. 1 : Close-up view of the CFD mesh around the airfoil.

The flow has two strong shocks that move on the upper and lower surfaces of the airfoil. Fig. 2 shows that the variations of the lift coefficient $c_l$ and the chordwise position of the shock on the upper surface $x_s$ obtained by the unsteady RANS simulation are in agreement with the experimental measurements. The turbulence model predicts the flow accurately as there is no massive separation or other more complex flow phenomena.

**2.** Fig. 3 and 4 show respectively the variation of the aerodynamic lift and moment coefficients, $c_l$ and $c_m$, obtained using the mean flow and the first fluid dynamic mode corresponding to the pitching frequency extracted by a Dynamic Mode

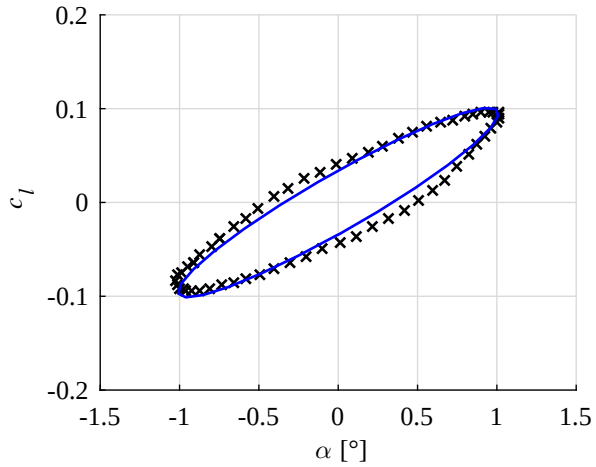


(a) Lift coefficient $c_l$

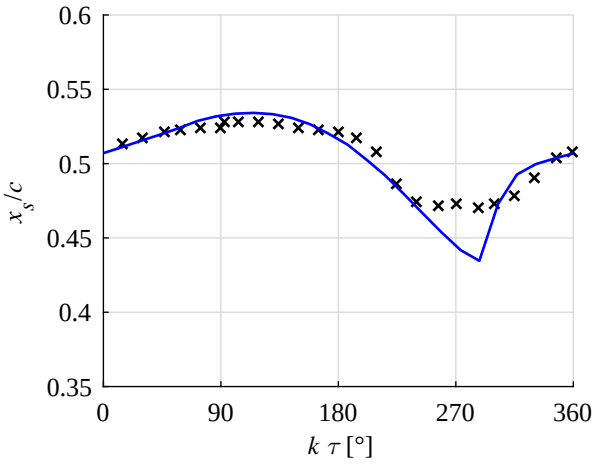


(b) Chordwise position of the shock on the upper surface $x_s$

Fig. 2 : Comparison of the unsteady RANS solution (blue line) with the experimental data of Davis [10] (black symbols) for the pitching NACA 64A010 case at reduced frequency $k = 0.202$.

Decomposition (DMD) of the unsteady RANS flow fields. The lift and moment coefficients calculated using a single flow dynamic mode are already in very good agreement with the unsteady RANS solutions even at forcing frequencies that can be considered high in the context of flutter problems.

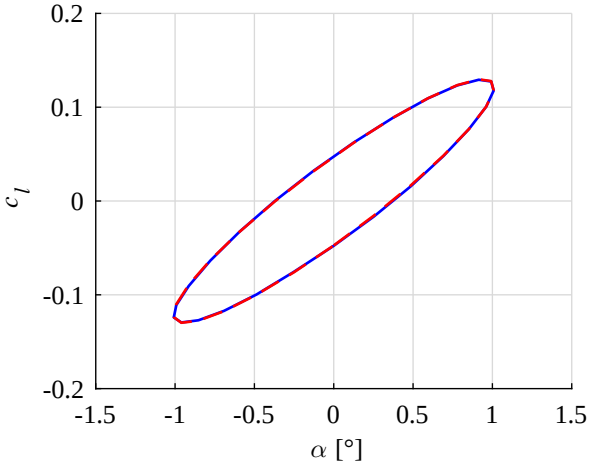


(a) $k = 0.1$

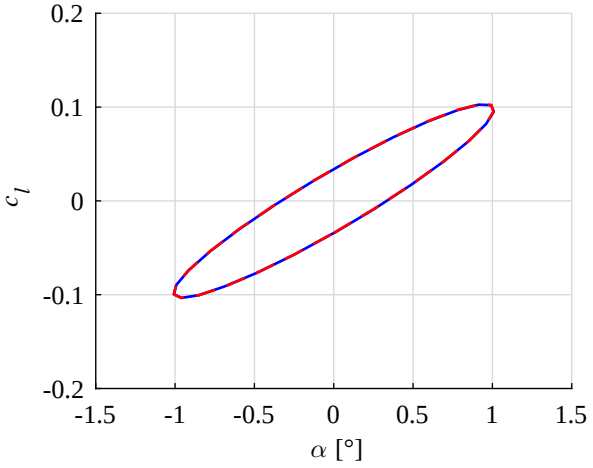


(b) $k = 0.202$

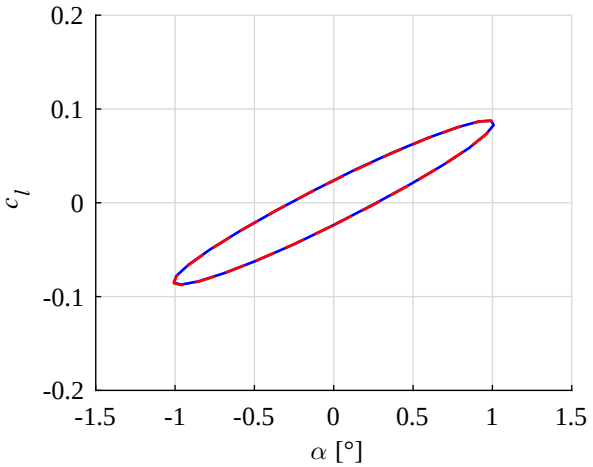


(c) $k = 0.3$

Fig. 3 : Comparison of the lift coefficient $c_l$ between the unsteady RANS solution (blue line) and the one-mode DMD representation (dashed red line) for the pitching NACA 64A010 case at three values of the reduced frequency $k$.

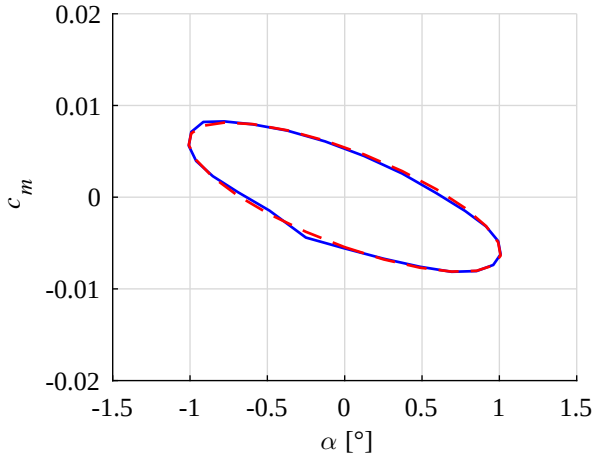


(a) $k = 0.1$

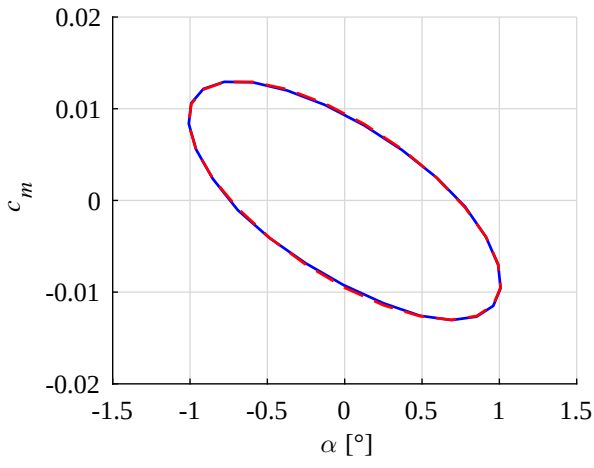


(b) $k = 0.202$

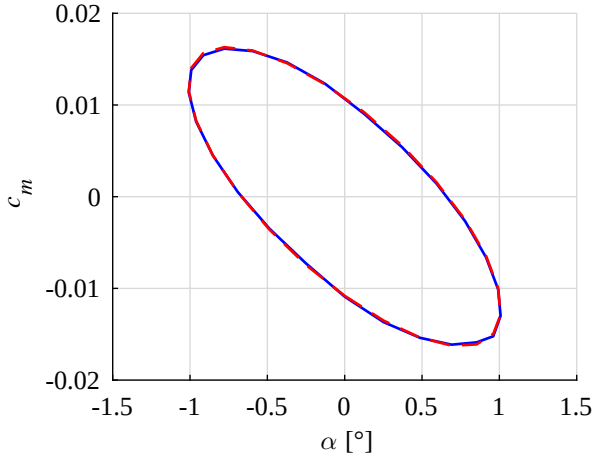


(c) $k = 0.3$

Fig. 4 : Comparison of the moment coefficient $c_m$ between the unsteady RANS solution (blue line) and the one-mode DMD representation (dashed red line) for the pitching NACA 64A010 case at three values of the reduced frequency $k$.

**3.** The proposed methodology computes the first flow dynamic modes at two nearby reduced frequencies, and then estimates the modes corresponding to other reduced frequencies through linear interpolation. This allows to account for the progressive changes in the mode shape with $k$ at a limited cost. As an example, in Fig. 5, the lift and moment coefficients for $k = 0.202$ estimated by the dynamic mode interpolation approach based on the first dynamic modes at $k = 0.1$ and 0.3 are compared to the corresponding results using the exact modes at $k = 0.202$ and the unsteady RANS solution. The dynamic mode interpolation approach provides good results, even with a single dynamic mode.

More generally, for the present case, interpolating from the solutions at $k = 0.1$ and 0.3 provides good estimations of the most dominant modes, and hence of the complete flow dynamics, over a large range of oscillation frequencies given that the frequency is not too far from the chosen reference frequencies. From a computational point of view, only two unsteady simulations are sufficient here for given flow conditions.

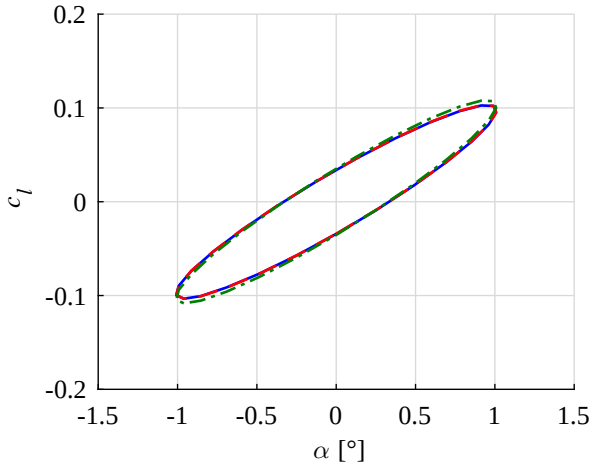


(a) Lift coefficient $c_l$

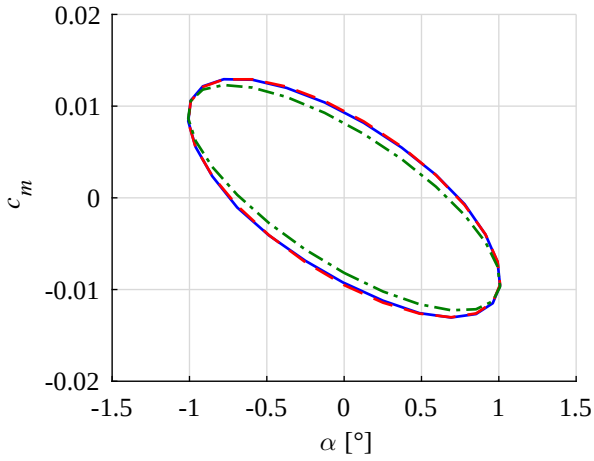


(b) Moment coefficient $c_m$

Fig. 5 : Comparison of the unsteady RANS solution (blue line), the one-mode DMD representation (dashed red line), and the present dynamic mode interpolation approach (dash-dot green line) based on the first dynamic modes at $k = 0.1$ and 0.3 for the pitching NACA 64A010 case at reduced frequency $k = 0.202$.

## 4 Application to a 2D transonic flutter calculation

In this section, the methodology is applied to the stability analysis of a 2D airfoil model in order to test its performance for predicting the onset of transonic flutter.

As illustrated in Fig. 6, the Isogai wing section model [15] consists in a 2D airfoil with two degrees of freedom; it can undergo a combination of pitching ($\alpha$) and plunging ($h$) motion. The aeroelatic equation for the system is given by

$$\mathbf{M}\begin{pmatrix}\ddot{h}(t)\\ \ddot{\alpha}(t)\end{pmatrix}+\mathbf{K}\begin{pmatrix}h(t)\\ \alpha(t)\end{pmatrix}=\begin{pmatrix}-l(t)\\ m(t)\end{pmatrix}, \quad (2)$$

where $\mathbf{M}$ and $\mathbf{K}$ are the mass and stiffness matrices of the structure, respectively, $l$ is the aerodynamic lift, and $m$ is the aerodynamic moment about the elastic axis. The geometry is a NACA 64A010 airfoil, which is the same as for the pitching airfoil test case studied in Section 3. All the structural parameters shown in Fig. 6, on which the mass and stiffness matrices directly depend, are known from Isogai [15].

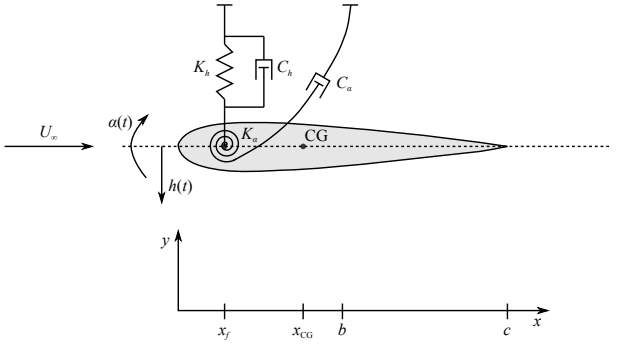


Fig. 6 : Typical two-degree-of-freedom airfoil aeroelastic model. (Adapted from Reference [16].)

The aerodynamic forces depend on the dynamics of the system and are not explicitly known because of the nonlinearity of the problem. Assuming a sinusoidal motion of the system and a resulting sinusoidal lift and moment, and decoupling the plunging and pitching motion for constant small amplitudes, the aeroelastic equation in the frequency domain for the system can be written in the general form [6, 17, 18]:

$$\left(-\left(\frac{kU_\infty}{b}\right)^2\mathbf{M}+\mathbf{K}-\frac{1}{2}\rho U_\infty^2\mathbf{Q}_1(k)\right)\mathbf{r}(k) = \frac{1}{2}\rho U_\infty^2\mathbf{Q}_0, \quad (3)$$

where

- $U_\infty$ is the free-stream velocity.
- $\rho$ is the air density.
- The components of the frequency-domain generalized aerodynamic force matrix are $\mathbf{Q}(k)=1/2\rho U_\infty^2(\mathbf{Q}_0(0)+\mathbf{Q}_1(k))$:

$$\mathbf{Q}_1(k)=\begin{pmatrix}\frac{-c\,\hat{c}_{l_{\text{plunge}}}(k)}{\hat{h}} & \frac{-c\,\hat{c}_{l_{\text{pitch}}}(k)}{\hat{\alpha}}\\ \frac{c^2\,\hat{c}_{m_{\text{plunge}}}(k)}{\hat{h}} & \frac{c^2\,\hat{c}_{m_{\text{pitch}}}(k)}{\hat{\alpha}}\end{pmatrix} \quad (4)$$

$$\mathbf{Q}_0=\begin{pmatrix}-c\,\bar{c}_{l_{\text{plunge}}} & -c\,\bar{c}_{l_{\text{pitch}}}\\ c^2\,\bar{c}_{m_{\text{plunge}}} & c^2\,\bar{c}_{m_{\text{pitch}}}\end{pmatrix}, \quad (5)$$

  where $\hat{c}_{l_{\text{plunge}}}$ and $\hat{c}_{m_{\text{plunge}}}$ denote the lift and moment coefficient amplitudes due to a plunging motion of amplitude $\hat{h}$, $\hat{c}_{l_{\text{pitch}}}$ and $\hat{c}_{m_{\text{pitch}}}$ represent those due to a pitching motion of amplitude $\hat{\alpha}$, and $\bar{c}_{l_{\text{plunge}}}$, $\bar{c}_{m_{\text{plunge}}}$, $\bar{c}_{l_{\text{pitch}}}$, and $\bar{c}_{m_{\text{pitch}}}$ denote the associated mean values. Matrix $\mathbf{Q}$ is complex and depends on $k$.

- The vector of generalized coordinates in the frequency domain is

$$\mathbf{r}(k)=\begin{pmatrix}\hat{h}\\ \hat{\alpha}\end{pmatrix}e^{ik\tau}. \quad (6)$$

The dynamic mode interpolation approach is used for the aerodynamic loads. The aerodynamic parameters $\hat{c}_{l_{\text{pitch}}}$, $\hat{c}_{m_{\text{pitch}}}$, $\bar{c}_{l_{\text{pitch}}}$, and $\bar{c}_{m_{\text{pitch}}}$ are calculated using the same steps:

**1.** For given flow conditions (Reynolds number $Re$ and Mach number $M$), two unsteady RANS or Euler simulations are carried out for a forced pitching motion at two reference reduced frequencies $k = 0.1$ and $0.3$. A small pitching amplitude is sufficient for flutter analysis. The pitching amplitude $\hat{\alpha}$ is set to $1^\circ$ here.

**2.** The next step consists in obtaining the first dynamic modes through DMD of the unsteady RANS or Euler flow fields.

**3.** The first dynamic pressure mode is then obtained at any other frequency through interpolation between the two reference frequencies. From the interpolated pressure modes, the lift and moment coefficients are calculated at any frequency and normalized by the amplitude $\hat{\alpha}$ of the imposed pitching motion.

The entire procedure can be repeated for the plunging motion. The plunging amplitude $\hat{h}$ is set to $0.1c$ here. Finally, matrix $\mathbf{Q}$ can thus be computed for a given Mach number using only four unsteady RANS simulations.

The flutter boundary at $Re = 6 \times 10^6$ obtained by applying the *p-k* method in conjunction with the proposed dynamic mode interpolation methodology is represented by the blue circles in Fig. 7. Comparison with results from the literature based on unsteady RANS simulations of the full Fluid-Structure Interaction (FSI) problem [19] demonstrates that the present approach provides a very good estimate of the flutter boundary. In particular, the transonic dip is well captured. Very good predictions are also obtained for the inviscid case (based on Euler simulations), for which more reference data is available for comparison, as shown in Fig. 8. Similar accuracy is achieved as with higher-fidelity methods, but at a much lower computational cost.

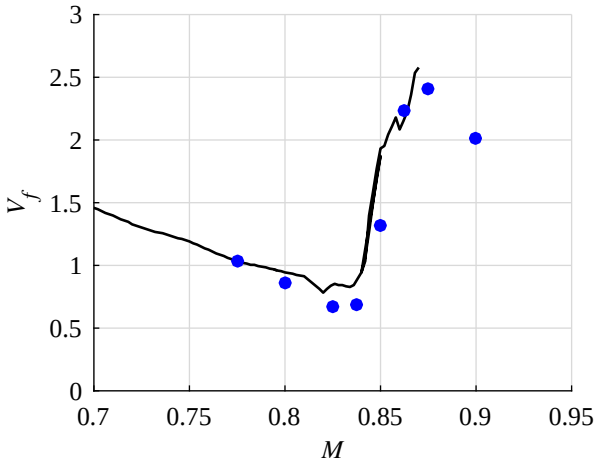


Fig. 7 : Flutter boundary (flutter speed index $V_f$ as a function of the Mach number $M$) for the Isogai case obtained by the present approach based on viscous flow modeling at $Re = 6 \times 10^6$ (blue circles) and compared to the time-accurate aeroelastic simulations using the RANS equations of Timme *et al.* [19] (black line).

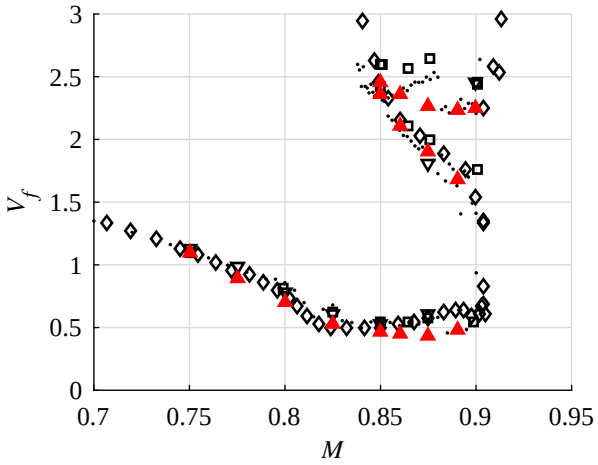


Fig. 8 : Flutter boundary (flutter speed index $V_f$ as a function of the Mach number $M$) for the Isogai case obtained with the present approach based on inviscid flow modeling (red triangles) and compared to time-accurate aeroelastic simulations using the Euler equations: Timme and Badcock [19] (dots), Yang *et al.* [20] (squares), Hall *et al.* [21] (diamonds), Alonso *et al.* [16] (downward-pointing triangles).

Fig. 9 compares the viscous and inviscid flutter boundaries predicted by the *p-k* method using the proposed methodology. It can be seen that viscosity reduces the transonic dip, suppresses the fold in the flutter boundary and the higher-frequency flutter mode present in the inviscid case. If the Reynolds number of the flow is reduced, it can be seen that the transonic dip is shifted to higher flutter speed. To further highlight the advantage of the method, the results obtained with a typical linear panel method are also shown for comparison in Fig. 9. Although such methods are very fast, they fail to capture the transonic dip because they do not model the critical unsteady phenomena charaterizing transonic flows (e.g., shock oscillations).

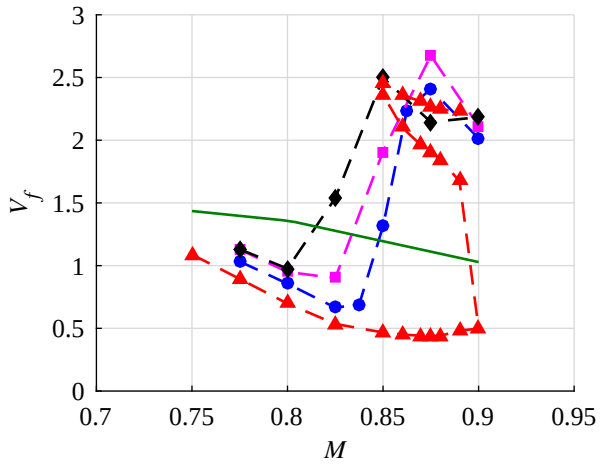


Fig. 9 : Flutter boundary (flutter speed index $V_f$ as a function of the Mach number $M$) for the Isogai case obtained with the present approach based on viscous flow modeling at $Re = 6 \times 10^6$ (blue circles), $Re = 1 \times 10^6$ (magenta squares), $Re = 1 \times 10^5$ (black diamonds) and inviscid flow modeling (red triangles). The green line represents the results from the linear thin-airfoil theory [1].

Fig. 10 shows the evolution of the system damping ratios for $M = 0.85$, which allows the characterisation of the subcritical behavior of the system. There are significant differences between the viscous and inviscid cases. In the viscous case, only the plunging mode becomes unstable and the flutter mechanism is less abrupt compared to the inviscid case: the damping drops less quickly to zero. Moreover, the flutter speed index obtained with viscous flow modeling is much higher than the first flutter point present in the inviscid case.

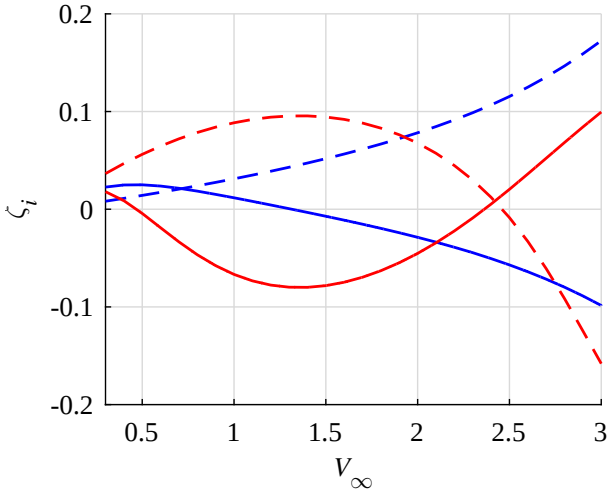


Fig. 10 : Evolution of the damping ratios $\zeta_i$ associated with the plunge (continuous line) and pitch (dashed line) degrees of freedom obtained by the present approach for $M = 0.85$. The blue curves are the viscous flow results at $Re = 6 \times 10^6$ and the red curves are the inviscid flow results.

## 5 Conclusions

The proposed unsteady aerodynamic modeling methodology based on dominant fluid dynamic mode interpolation has been demonstrated on the Isogai wing, using both inviscid and viscous calculations. The methodology is able to properly predict the flow response to small periodic harmonic oscillations of the structure for a large range of reduced frequencies through the interpolation of the first fluid dynamic modes computed at two nearby oscillation frequencies. The methodology takes into account the moving shocks and their interactions with the viscous boundary layer.

The proposed methodology can be used with the *p-k* flutter solution method. It provides a very good estimate of the flutter boundary for the 2D Isogai airfoil validation case, but at a lower computational cost than the traditional higher-fidelity Fluid-Structure Interaction (FSI) simulations. Only four simulations are required per Mach number to determine the flutter speed. The methodology being relatively fast, sensitivity analysis (e.g., effect of Reynolds number variation) is feasible. The methodology may also use the same reference aerodynamic solutions for slightly different mass and stiffness matrices, which is an important advantage to study the flutter characteristics of slightly different configurations.

## 6 Acknowledgements

The authors gratefully acknowledge the aerospace company Embraer S.A. for supporting this research. Computational resources have been provided by the Consortium des Équipements de Calcul Intensif (CÉCI), funded by the Fonds de la Recherche Scientifique de Belgique (F.R.S.-FNRS) under Grant No. 2.5020.11.

## References

[1] Oddvar O Bendiksen. Review of unsteady transonic aerodynamics: theory and applications. *Progress in Aerospace Sciences*, 47(2):135–167, 2011.

[2] Gareth A Vio, Grigorios Dimitriadis, Jonathan E Cooper, Ken J Badcock, Mark A Woodgate, and Abdul M Rampurawala. Aeroelastic system identification using transonic CFD data for a wing/store configuration. *Aerospace Science and Technology*, 11(2):146–154, 2007.

[3] Kenneth C Hall, Jeffrey P Thomas, and William S Clark. Computation of unsteady nonlinear flows in cascades using a harmonic balance technique. *AIAA journal*, 40(5):879–886, 2002.

[4] Sravya Nimmagadda, Thomas D Economon, Juan J Alonso, and Carlos R Ilario da Silva. Robust uniform time sampling approach for the harmonic balance method. In *46th AIAA Fluid Dynamics Conference*, page 3966, 2016.

[5] William P Rodden and E Dean Bellinger. Aerodynamic lag functions, divergence, and the british flutter method. *Journal of Aircraft*, 19(7):596–598, 1982.

[6] H. Güner, D. Thomas, G. Dimitriadis, and V.E. Terrapon. Unsteady aerodynamic modeling methodology based on dynamic mode interpolation for transonic flutter calculations. *Submitted to Journal of Fluids and Structures*, 2018.

[7] Peter J Schmid. Dynamic mode decomposition of numerical and experimental data. *Journal of Fluid Mechanics*, 656:5–28, 2010.

[8] Mihailo R Jovanović, Peter J Schmid, and Joseph W Nichols. Sparsity-promoting dynamic mode decomposition. *Physics of Fluids*, 26(2):024103, 2014.

[9] Hüseyin Güner, Grigorios Dimitriadis, and Vincent Terrapon. Research on fast aeroelastic modeling methods for the transonic regime. In *Proceedings of the International Forum on Aeroelasticity and Structural Dynamics, IFASD 2017*, pages Paper–IFASD, 2017.

[10] Sanford S Davis. NACA 64A010 (NASA Ames model) oscillatory pitching. *AGARD Report*, 702, 1982.

[11] PRaA Spalart and S1 Allmaras. A one-equation turbulence model for aerodynamic flows. In *30th aerospace sciences meeting and exhibit*, page 439, 1992.

[12] Francisco Palacios, Michael R Colonno,

Aniket C Aranake, Alejandro Campos, Sean R Copeland, Thomas D Economon, Amrita K Lonkar, Trent W Lukaczyk, Thomas WR Taylor, and Juan J Alonso. Stanford university unstructured (su2): An open-source integrated computational environment for multi-physics simulation and design. *AIAA Paper*, 287:2013, 2013.

[13] Francisco Palacios, Thomas D Economon, Aniket C Aranake, Sean R Copeland, Amrita K Lonkar, Trent W Lukaczyk, David E Manosalvas, Kedar R Naik, A Santiago Padrón, Brendan Tracey, et al. Stanford university unstructured (su2): Open-source analysis and design technology for turbulent flows. *AIAA paper*, 243:13–17, 2014.

[14] Thomas D Economon, Francisco Palacios, Sean R Copeland, Trent W Lukaczyk, and Juan J Alonso. Su2: an open-source suite for multiphysics simulation and design. *AIAA Journal*, 2015.

[15] Koji Isogai. On the transonic-dip mechanism of flutter of a sweptback wing. *AIAA journal*, 17(7):793–795, 1979.

[16] Juan Alonso and Antony Jameson. Fully-implicit time-marching aeroelastic solutions. In *32nd Aerospace Sciences Meeting and Exhibit*, page 56, 1994.

[17] Grigorios Dimitriadis. *Introduction to Nonlinear Aeroelasticity*. John Wiley & Sons, 2017.

[18] Grigorios Dimitriadis, NF Giannelis, and GA Vio. A modal frequency-domain generalised force matrix for the unsteady vortex lattice method. *Journal of Fluids and Structures*, 76:216–228, 2018.

[19] S Timme and KJ Badcock. Transonic aeroelastic instability searches using sampling and aerodynamic model hierarchy. *AIAA journal*, 49(6):1191–1201, 2011.

[20] Shuchi Yang, Zhichao Zhang, Feng Liu, Shijun Luo, Her-Mann Tsai, and David Schuster. Time-domain aeroelastic simulation by a coupled euler and integral boundary-layer method. In *22nd Applied Aerodynamics Conference and Exhibit*, page 5377, 2004.

[21] Kenneth C Hall, Jeffrey P Thomas, and Earl H Dowell. Proper orthogonal decomposition technique for transonic unsteady aerodynamic flows. *AIAA journal*, 38(10):1853–1862, 2000.

## 7 Contact Author Email Address

hguner@uliege.be

## Copyright Statement